Transverse and Axial Beam Shaping in the Non-Paraxial Domain

Stephen M. Kuebler*[a,b] and Toufic G. Jabbour[a]
[a]CREOL, The College of Optics and Photonics and [b]Department of Chemistry
University of Central Florida, Orlando, Florida, 32618, USA

ABSTRACT

The design of beam-shaping pupil filters most commonly employs the scalar theory of diffraction, which does not accurately describe the focal field distribution under high numerical aperture focusing. To account for the full vector character of the field, we have developed computational algorithms for designing phase-only pupil filters that incorporate the electromagnetic theory of diffraction. These algorithms use the method of generalized projects or particle swarm optimization to generate phase-filter solutions based on a targeted focal field irradiance distribution. Computational results are presented that demonstrate how these procedures can be used to design phase filters that re-shape the transverse beam, or achieve axial super-resolution for a single focused spot. The methods can be applied in the design of beam-shaping and superresolving optics used for imaging, direct laser writing, and lithography.

Keywords: Laser beam shaping, superresolution, vector diffraction theory, diffractive optics, pupil filters.

1. INTRODUCTION

Diffractive optical elements (DOEs) are pupil filters (Fig. 1) that can be used to modify the amplitude, phase, and polarization of an incident beam so that it focuses into an irradiance distribution – or point spread function (PSF) – that is modified relative to the diffraction limited pattern.[1-3] Incorporating DOEs into optical systems is increasingly common as they can greatly enhance performance in a wide range of applications, including optical lithography, laser-based materials processing, direct laser writing, surgical applications, and optical data storage.[4] The term "beam shaping" is most frequently applied to situations in which a DOE is used to modify the irradiance distribution within the geometric focal plane (transverse PSF) without concern for accompanying changes in the direction of focused beam propagation (the axial direction). Applications of axial beam shaping include lengthening the axial PSF (extended depth of focus) or decreasing the axial extent below the diffraction limit to achieve axial superresolution. Modifying the PSF, particularly superresolving transversely or axially, creates undesirable side-lobes and/or re-distributes optical power outside of the region of interest. Because an arbitrary PSF is not necessarily a solution to the wave equation, it may not be possible to generate the targeted irradiance distribution exactly. Designing a beam shaping DOE is thus an inverse optimization problem that involves finding a solution that offers a satisfactory compromise between formation of the targeted PSF and minimization of unwanted features. The problem is ill-posed because the form of the DOE that most closely yields the targeted PSF may not be unique. Given that a two-dimensional DOE affects the entire three-dimensional (3D) irradiance distribution, transverse and axial features in the PSF are inextricably linked, so simultaneously engineering the axial and transverse PSF, or 3D beam shaping, is even more challenging.

Many excellent scalar techniques have been reported for designing beam shaping DOEs. These are based on methods that include geometric mapping,[5, 6] analytical solution,[7] iterative processes,[8-11] and genetic optimization.[12] Although exceptional results have been achieved with these algorithms, they are all based on scalar diffraction theory, and as such are only valid in the paraxial domain of diffractive optics.[13] For systems with high numerical aperture (*NA*), depolarization effects are significant,[14] so vectorial diffraction theory must be used in the DOE design process. This becomes particularly challenging because the overall beam shape is determined by the summed intensity of the *x*-, *y*-, and *z*-polarized fields. Although the field components are orthogonal, they are not entirely independent because each is reshaped by a common DOE. As a result, the DOE must be designed so that it collectively reshapes I_x, I_y, and I_z such that their sum $I_x + I_y + I_z = I_f$ tends toward I_t. Given that high-*NA* systems are increasingly employed in frontier technologies, further applications of beam shaping require the development of accurate vectorial methods for transverse,

*kuebler@mail.ucf.edu; phone +1-407-823-3720; fax +1-407-823-2522; http://npm.creol.ucf.edu

Laser Beam Shaping X, edited by Andrew Forbes, Todd E. Lizotte, Proc. of SPIE Vol. 7430, 743002 · © 2009 SPIE · CCC code: 0277-786X/09/$18 · doi: 10.1117/12.827475

axial, and 3D beam shaping. This work overviews several vectorial beam shaping algorithms we have developed for the design of axially superresolving and transverse-field shaping phase-only DOEs.

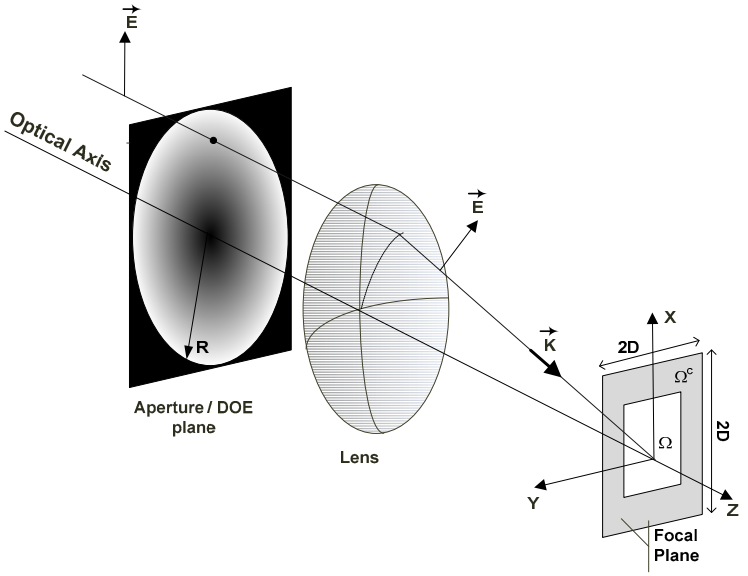

Fig. 1. Optical setup of the beam shaping problem. The aperture represents the input pupil of the high-*NA* objective lens. For transverse beam shaping, the geometric focal plane can be divided into two regions. Area Ω represents the region of interest that contains and bounds the targeted transverse profile. Its complement Ω^c represents the remainder of the focal plane.

2. THEORY

The optical geometry considered throughout this work (Fig. 1) consists of the DOE and an aberration free high-*NA* lens having focal length *f*. The two are positioned such that their optical axes are collinear with the *z*-axis of a Cartesian coordinate system whose origin is located at the geometric focus of the lens. The numerical aperture of the lens is *NA* = 1.4. Monochromatic linearly polarized plane waves having a vacuum wavelength of λ = 800 nm and electric field vector parallel to the *x*-axis propagate along the *z*-axis, passing through the DOE and entering the pupil of the lens. The light focuses into a medium of refractive index n = 1.516. In the absence of the DOE, this situation is consistent with common applications of high-*NA* oil-immersion objective lenses.

Starting from the vector diffraction integrals,[15, 16] the electric field at an arbitrary point $P(x_f, y_f, z_f)$ within the geometric focal plane (z = 0) represented as[17]

$$\begin{bmatrix} E_x \\ E_y \\ E_z \end{bmatrix} = -i\frac{fE_{in}}{2\pi} \iint_{\sqrt{k_x^2+k_y^2} \le k_{\max}} T(k_x,k_y) e^{i\Phi(k_x,k_y)} \sqrt{\frac{k_z}{k_t}} \frac{1}{k_z} \begin{bmatrix} \dfrac{k_x^2(k_z/k_t)+k_y^2}{k_x^2+k_y^2} \\ \dfrac{k_x k_y(k_z/k_t-1)}{k_x^2+k_y^2} \\ -\dfrac{k_x}{k_t} \end{bmatrix} \times e^{i(k_x x_f + k_y y_f)} dk_x dk_y \,, \tag{1}$$

and the corresponding irradiance is $I = (1/2)nc\varepsilon_0|\boldsymbol{E}|^2$. The speed of light and electric permittivity in vacuum are c and ε_0, respectively. A transversely shaped beam is the spatial map of the focused irradiance $I_f(x_f, y_f)$ for all $P(z = 0)$ The wave number is $k_t = 2\pi/\lambda = [k_x^2 + k_y^2 + k_z^2]^{1/2}$, with k_x, k_y, and k_z being the plane wave components, and λ is the wavelength within the medium. The *NA* of the lens system sets $k_{\max} = k_t NA/n$. The function $T(k_x, k_y)\exp[i\Phi(k_x, k_y)]$ describes the

transmission amplitude (T) and phase (Φ) of the DOE. The amplitude of the incident electric field E_{in} is assumed to be spatially constant, so this term is brought outside the integral. The focal plane can be divided into a region of interest Ω and its complement Ω^c. A targeted transverse beam shape I_t, such as a top-hat distribution, can be thought of as wholly contained and bounded by Ω.

If the DOE is assumed to be radially symmetric, the vector diffraction integrals may be expressed in a cylindrical coordinate system. The electric field distribution at point $P(r, z, \varphi)$ near the geometric focal is given by[16, 18]

$$E(r,z,\varphi) = iA\left[\left(I_0 + I_2\cos 2\varphi\right)\hat{\mathbf{x}} + \left(I_2 \sin 2\varphi\right)\hat{\mathbf{y}} - i\left(2I_1\cos\varphi\right)\hat{\mathbf{z}}\right]. \tag{2}$$

$I_{0,1,2}$ are integrals evaluated over the aperture half-angle θ as

$$I_0(z,r) = \int_0^\alpha t(\theta)\sqrt{\cos\theta}\,\sin\theta(1+\cos\theta)J_0\left(k_t r\sin\theta\right)\exp\left(ik_t z\cos\theta\right)d\theta, \tag{3}$$

$$I_1(z,r) = \int_0^\alpha t(\theta)\sqrt{\cos\theta}\,\sin^2\theta J_1\left(k_t r\sin\theta\right)\exp\left(ik_t z\cos\theta\right)d\theta, \tag{4}$$

$$I_2(z,r) = \int_0^\alpha t(\theta)\sqrt{\cos\theta}\,\sin\theta(1-\cos\theta)J_2\left(k_t r\sin\theta\right)\exp\left(ik_t z\cos\theta\right)d\theta. \tag{5}$$

Variables r and z represent the radial and axial coordinates, respectively. Angle φ is that subtended by the electric field vector of the incident field and the meridian plane in which the field distribution is calculated. The maximum aperture half-angle angle $\alpha = \arcsin(NA/n)$, is determined by the numerical aperture of the lens and n. The constant $A = \pi E_{in} f/\lambda$. In this representation, the DOE complex transmission function is described by $t(\theta)$. If we are concerned with only the axial field distribution, $E_{\text{axial}}(z)$, we may set $r = 0$ in Eqs. 2 – 5, giving

$$E_{axial}(z) = iA\int_{q(0)}^{q(\alpha)} t(q)\sqrt{q}\,(1+q)\exp(ikzq)\,dq, \tag{6}$$

where $q = \cos\theta$. The normalized radius of the aperture, r, and q are related by $r = n(1 - q^2)^{1/2}/NA$.

3. OPTIMIZATION METHODS

3.1 Method of generalized projections

Given a set of solution constraints C_γ ($\gamma = 1,2,\ldots, \eta$), the Method of Generalized Projections (MGP) seeks a solution function S by iteratively projecting onto constraints according to $S_{\chi+1} = \mathbf{P}_1\mathbf{P}_2\ldots\mathbf{P}_n S_\chi$,[19] where χ is an iteration index, S_0 is an initial function, and $\mathbf{P}_\gamma$ is a projection operator that maps S onto its nearest neighbor in C_γ. In the context of beam shaping, each solution S corresponds to an irradiance distribution I_χ calculated in iteration χ using the vector diffraction integrals based on a trial DOE complex transmission. The constraints define the targeted profile, I_t, and may include terms relevant to the DOE complex transmission function, such as a restriction to binary phase-only DOE profiles. During each iteration, the suitability of the trial DOE solution is judged based on a fitness parameter. When constraints are inconsistent (meaning all cannot be satisfied simultaneously), the MGP yields a solution that most nearly satisfies the set of requirements.[19]

3.2 Particle swarm optimization

PSO is a nature-inspired method for optimizing nonlinear functions motivated by the idea that individuals in a population can evolve based on information gathered through their own experience and that of the group.[20] The individuals and the group are referred to as *particles* and the *swarm*, respectively. During optimization a randomly generated swarm searches the solutions space for the "best" solution. Each iteration, solutions are compared using a fitness parameter, and the position and velocity of the i-th particle are updated based on the best solution it found, b_i, and the overall best position b_G found by the swarm. The comparison and update are applied to all particles and repeated

over many iterations. The update process is then an aggregated acceleration of the *i*-th particle towards the best position identified by the ensemble.

4. AXIAL BEAM SHAPING

Previously we reported how PSO can be applied for designing *N*-zone radially symmetric binary phase-only DOEs that axially superresolve the PSF.[21] The on-axis irradiance, I_{axial}, for diffraction-limited focusing (no DOE) consists of a main lobe that peaks at the focal plane and side lobes that decrease in magnitude with distance from the focal plane. A properly designed DOE can superresolve the axial width of the main lobe, but this is accompanied by an increase in intensity of the side lobes. The degree of superresolution achieved with a given DOE can be characterized by parameter *G*, defined as the full-width at half-maximum (FWHM) of superresolved I_{axial} divided by that of diffraction limited I_{axial}. The magnitude of side-lobe increase can be quantified using a second parameter *M*, defined as the ratio of the peak intensity of the largest side lobe versus that of the main lobe. For many applications, large side lobes are not tolerable, so axial superresolution also requires optimizing the degree of achievable superresolution against the associated increase in side lobe intensity. Axial super-resolution can be viewed as a combinatorial problem in which fields originating from multiple zones of the DOE are added or subtracted to give E_{axial} having minimum *G* for a fixed limit on side lobe intensity M_{lim}.

In our application of PSO, the binary phase DOE evaluated consisted of 100 equal-width zones, corresponding to an overall solutions space of $2^{N-1} \approx 6.3 \times 10^{29}$ unique DOEs. The solutions space was searched by a swarm of 40 particles to find that DOE which offers the best superresolution (lowest *G*) and side lobe intensity constrained to $M \le M_{lim}$. The position of each particle within the space corresponds to a trial DOE. For each trial DOE, Eq. 6 was to used to calculate I_{axial}, *G*, and *M*. The position and velocity of each particle were then updated based on each particle's best solution (lowest *G* and $M \le M_{\text{lim}}$) and the overall best solution found by the swarm. The process was continued through 10,000 iterations.

Figure 2 shows the PSF generated by a DOE optimized with $M_{lim} = 0.5$. The central lobe FWHM is decreased by 34% relative to the diffraction-limited pattern, and the relative side lobe intensity is held below $M = 0.5$. To our knowledge this is the highest single-beam axial super-resolution calculated for a phase DOE with the given limit on side lobe intensity. Interestingly, the transverse FWHM of the central lobe increases by only 5% with respect to the diffraction limit, so lateral resolution is not sacrificed. The combined effect of axial super-resolution and minimal transverse broadening causes the central lobe to become more spherical. The ratio of the transverse to axial FWHM is 0.78. A more spherical PSF is desirable for many focused laser applications, such as multi-photon imaging and direct laser writing.

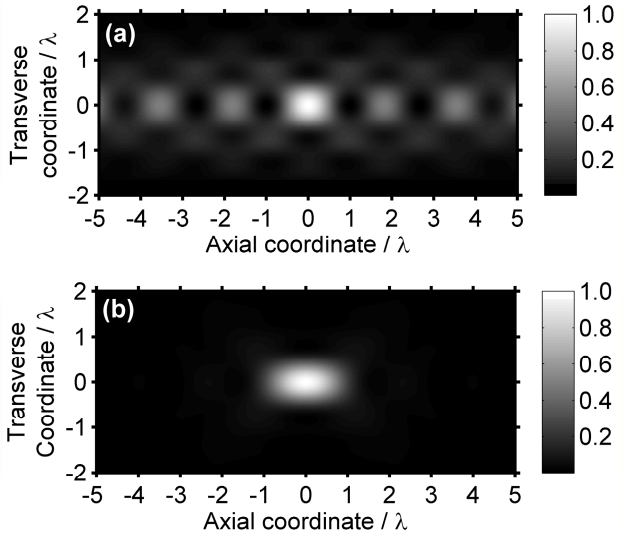

Fig. 2. PSF within the plane of incident polarization generated by (**a**) the axially super-resolving DOE obtained with PSO ($G = 0.66$, $M = 0.50$) and (**b**) for diffraction limited focusing (no DOE).

Previously, we reported the first vectorial algorithm for optimizing G and M based on the Method of Generalized Projections (MGP).[22] Although that method yields excellent results, it is not guaranteed to find the global solution because MGP is susceptible to "traps" and "tunnels" that can cause the algorithm to stagnate in local minima. The best DOE found using MGP offers $G = 0.71$ and $M = 0.52$. It is noteworthy that PSO outperforms MGP by finding a solution that offers both higher super-resolution and smaller side lobes. This can be attributed to the well known ability of PSO to avoid becoming trapped in local minima.[20, 23]

5. TRANSVERSE BEAM SHAPING

Many applications require re-shaping the transverse profile of a focused laser beam using a DOE. But doing so under high-*NA* conditions presents considerable challenge because the vector character of the field cannot be neglected. Even in the simplest case of a linearly polarized input field, high-*NA* focusing directs significant optical power into the other two field polarizations. For example, evaluating Eq. 1 and integrating I_x, I_y, and I_z over the entire focal plane shows that their fractional power content is 0.74, 0.01 and 0.25, respectively. So, high-*NA* beam shaping requires that we identify a DOE phase function Φ that generates a focal plane field distribution such that the sum of the *x*-, *y*-, and *z*-polarized irradiance $I_x + I_y + I_z = I_f$, matches the targeted irradiance I_t for all positions in the focal plane. An exact match is generally not possible because it is not known *a priori* that arbitrary I_t is a solution to the wave equation.[11] The problem is further complicated because Φ affects each of E_x, E_y, and E_z, so the field components are not truly independent. This problem cannot be solved analytically, so iterative numerical techniques must be employed. MGP is particularly well suited to this type of problem because it can find solutions that closely satisfy sets of inconsistent and non-physical constraints.[24]

We have shown how the MGP can be applied to vectorial transverse beam shaping in the design of analog phase-only DOEs for use under high-*NA* focusing.[17] For many applications the optimum transverse irradiance distribution consists of a flat-top profile having a defined geometry within the focal plane. We demonstrated our vectorial transverse beam shaping algorithm by applying it to the problem of re-shaping a circularly apodized flat-top input beam into a focused square flat-top irradiance distribution. The targeted intensity in the focal plane is given by:

$$I_t = \{1 \text{ for } (\xi,\eta) \in \Omega; \quad 0 \text{ for } (\xi,\eta) \in \Omega^c\}, \tag{7}$$

where ξ, η are normalized coordinates within the focal plane, and the limits of Ω are set to $-0.25 \le \xi, \eta \le 0.25$. The diffraction integrals in Eq. 1 are used to interrelate the DOE phase profile and the resulting vectorial electric field in the focal plane. The integrals are evaluated using the chirp-z transform[25] to improve computational speed and accuracy. In each iteration, the constraint associated with the targeted irradiance distribution is applied only to the *x*-polarized field using

$$E_x(\xi,\eta) = \sqrt{\frac{2}{nc\varepsilon_0}\left[\gamma I_t(\xi,\eta) - I_y(\xi,\eta) - I_z(\xi,\eta)\right]}\exp[i\phi_x(\xi,\eta)] \quad \text{for } (\xi,\eta) \in \Omega, \tag{8}$$

whereas the following are left unchanged: $|E_x(\xi, \eta)|$ outside Ω; $|E_y(\xi, \eta)|$ and $|E_z(\xi, \eta)|$ across all $\Omega + \Omega^c$; and the phases $\phi(\xi, \eta)$ of all field components in $\Omega + \Omega^c$. This approach takes into account the effect of the DOE on all field components in the focal plane and directs the DOE complex transmission toward a form that satisfies Eq. 7. The scalar γ augments $|E_x(\xi, \eta)|$ in Ω relative to that in Ω^c. This operation provides a means for slowly pulling energy from Ω^c into Ω.[8] In this work $\gamma = 1.03$ was used for all iterations. The quality of the reshaped PSF is characterized each iteration in terms of the diffraction efficiency, κ, and uniformity error, δ.[26] The diffraction efficiency quantifies the fraction of total optical power directed into the targeted region of interest, and the uniformity error provides a measure of flatness in the intensity distribution across that region. High diffraction efficiency and low uniformity error are known to be mutually exclusive characteristics that must be considered jointly in optimizing DOEs. Iterative projection of constraints in the pupil and focal planes progressively forces the simulation toward a DOE phase profile that generates the targeted beam shape. This process continues until the algorithm converges to a suitable solution or until a fixed number of iterations are completed.

Figure 3 shows the normalized focal irradiance distributions of the three polarization components, I_x, I_y, and I_z, and the total focal irradiance distribution I_f generated by the DOE phase profile of Fig. 4. This DOE and the associated

irradiance distributions were obtained after 600 iterations. The overall beam shape is square as intended with $\delta = 7\%$ and $\kappa = 74.5\%$, indicating that it has good uniformity and power confinement within Ω.

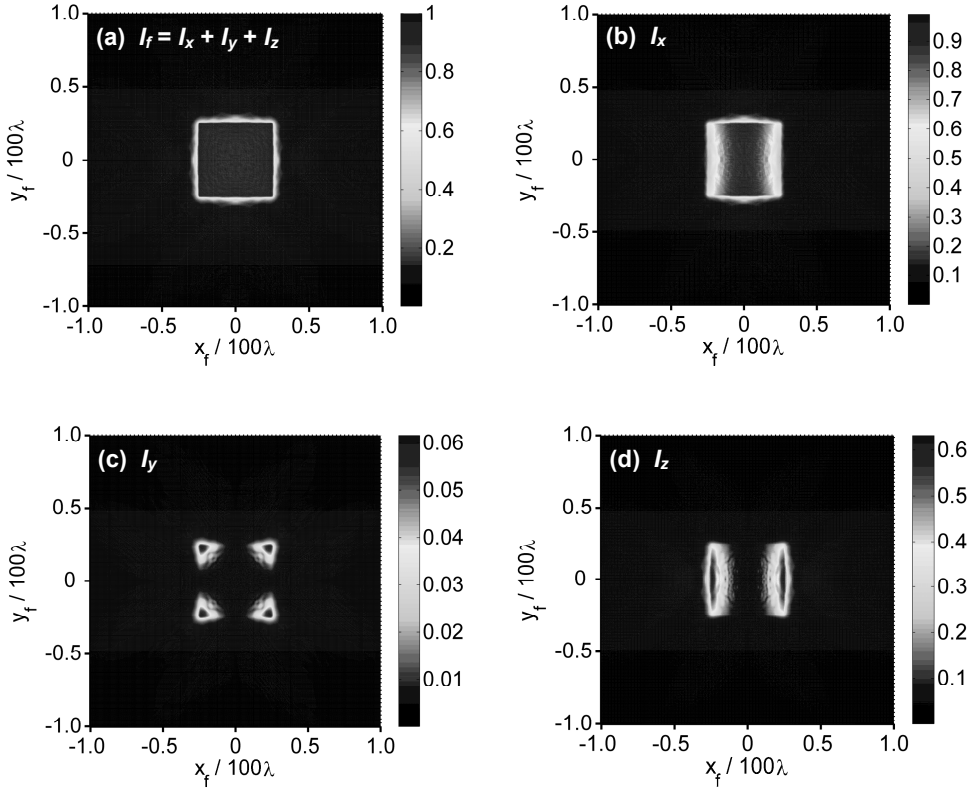

Fig. 3. (**a**) Calculated irradiance distribution resulting when a circularly apodized flat-top input beam is passed through the phase-only DOE shown in Fig. 4 and focused using a 1.4-*NA* objective. The DOE was designed to reshape the beam into a flat-top square irradiance pattern of area $50\lambda \times 50\lambda$. (**b**) - (**d**) Irradiances of the constituent *x*-, *y*-, and *z*-polarized components of the total field. Each profile is normalized to the peak of I_f.

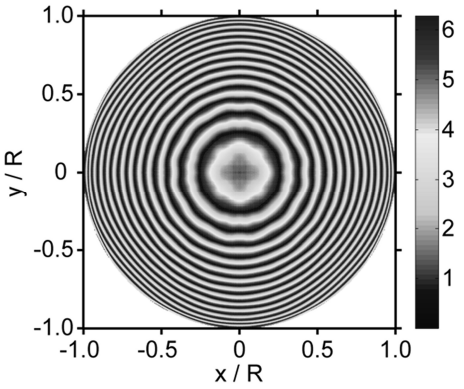

Fig. 4. DOE phase profile that generates the focal irradiance distributions shown in Fig. 3. The phase is plotted in units of radians.

In contrast, the irradiance distributions of the constituent polarizations are non-uniform. I_x most resembles the targeted profile, but appears doubly concave, as though squeezed along the *x*-axis. Although I_x is non-zero across the coordinate axes, I_y and I_z have node(s) at these positions where their field amplitudes drop to zero. I_y is most complex,

appearing approximately four-fold symmetric with power concentrated in the corners of Ω. I_z exhibits two-fold symmetry with a single nodal plane lying along the *y*-axis. The regions of high irradiance in I_y and I_z fill in around the edges of the *x*-polarized profile making the total irradiance distribution I_f uniform and square. These profiles show that the vector diffraction algorithm successfully generates a DOE for which all polarization components of the field are reshaped concurrently to achieve a targeted irradiance distribution under high-*NA* focusing.

6. CONCLUSION

Many of the optimization methods that have been so successfully applied for scalar beam shaping may also be used for vectorial DOE design, if the problem is suitably formulated. In this work, we have shown how the popular MGP algorithm can be used for transverse beam shaping. We have also introduced the PSO algorithm as a powerful new tool for optimizing DOEs, and we have shown how it can be used for axial beam shaping. One next logical step in this work would be to extend these methods for full three-dimensional vectorial field synthesis. Vectorial beam shaping remains a complex problem in part because fundamental knowledge is lacking of how focal field patterns and phase mask structure are related. Although the optimization tools discussed here can generate suitable solutions, they do not in and of themselves provide this insight. Further research, perhaps aided by these optimization methods, is necessary to improve our fundamental understanding of vectorial beam shaping.

REFERENCES

[1] C. Dorrer and J. D. Zuegel, "Design and analysis of binary beam shapers using error diffusion," *J. Opt. Soc. Am. B* **24**, pp. 1268-1275, (2007).

[2] V. Ramírez-Sánchez and G. Piquero, "Global beam shaping with nonuniformily polarized beams: a proposal," *Appl. Opt.* **45**, pp. 8902-8906, (2006).

[3] L. A. Romero and F. M. Dickey, "Lossless laser beam shaping," *J. Opt. Soc. Am. A* **13**, pp. 751-760, (1995).

[4] F. M. Dickey, S. C. Holswade, and D. L. Shealy, *Laser Beam Shaping Applications*, Taylor & Francis Group, Boca Raton, (2006).

[5] O. Bryngdhal, "Geometrical transformations in optics," *J. Opt. Soc. Am.* **64**, pp. 1092-1099, (1974).

[6] D. L. Shealy and S. H. Chao, "Geometric optics-based design of laser beam shapers," *Opt. Eng.* **42**, pp. 3123-3138, (2003).

[7] H. Aagedal, M. Schmid, S. Egner, J. Müller-Quade, T. Beth, and F. Wyrowski, "Analytical beam shaping with application to laser-diode arrays," *J. Opt. Soc. Am. A* **14**, pp. 1549-1553, (1997).

[8] M. Johansson and J. Bengtsson, "Robust design method for highly efficient beam-shaping diffractive optical elements using iterative-Fourier-transform algorithm with soft operations," *J. Mod. Optics* **47**, pp. 1385-1398, (2000).

[9] V. V. Kotlyar, P. G. Seraphimovich, and V. A. Soifer, "An iterative algorithm for designing diffractive optical elements with regularization," *Opt. Laser Eng.* **29**, pp. 261-268, (1998).

[10] J. S. Liu and M. R. Taghizadeh, "Iterative algorithm for the design of diffractive phase elements for laser beam shaping," *Opt. Lett.* **27**, pp. 1463-1465, (2002).

[11] F. Wyrowski, "Diffractive optical elements: iterative calculations of quantized, blazed phase structures," *J. Opt. Soc. Am. A* **7**, pp. 961-969, (1990).

[12] G. Zhou, X. Yuan, P. Dowd, Y. L. Lam, and Y. C. Chan, "Design of diffractive phase elements for beam shaping: hybrid approach," *J. opt. Soc. Am. A* **18**, pp. 791-800, (2001).

[13] M. Kuittinen, P. Vahimaa, M. Honkanen, and J. Turunen, "Beam shaping in the nonparaxial domain of diffractive optics," *Appl. Opt.* **36**, pp. 2034-2041, (1997).

[14] T. Jabbour and S. M. Kuebler, "Vector diffraction analysis of high numerical aperture focused beams modified by two- and three-zone annular multi-phase plates," *Opt. Express* **14**, pp. 1033-1043, (2006).

[15] E. Wolf, "Electromagnetic diffraction in optical systems I. An integral representation of the image field," *Proc. Royal Soc. A* **253**, pp. 349-357, (1959).

[16] R. Kant, "An analytical solution of vector diffraction for focusing optical systems with Seidal aberrations I. Spherical aberration, curvature of field, and distortion," *J. Mod. Optics* **40**, pp. 2293-2310, (1993).

[17] T. G. Jabbour and S. M. Kuebler, "Vectorial beam shaping," *Opt. Express* **16**, pp. 7203-7213, (2008).

[18] B. Richards and E. Wolf, "Electromagnetic diffraction in optical systems II. Structure of the image field in an aplanatic system," *Proc. Royal Soc. A* **253**, pp. 358-379, (1959).
[19] A. Levi and H. Stark, "Image restoration by the method of generalized projections with application to restoration from magnitude," *J. Opt. Soc. Am. A* **1**, pp. 932-943, (1984).
[20] J. Kennedy and R. C. Eberhart. "Particle swarm optimization." Conf.: IEEE Intl. Conf. Neural Networks, Perth, WA, Australia. IEEE, publ. (1995).
[21] T. G. Jabbour and S. M. Kuebler, "Particle swarm optimization of axially super-resolving binary phase diffractive optical elements," *Opt. Lett.* **33**, pp. 1533-1535, (2008).
[22] T. G. Jabbour, M. Petrovich, and S. M. Kuebler, "Design of axially super-resolving phase filters using the method of generalized projections," *Opt. Commun.*, pp. 2002-2011, (2008).
[23] J. Kennedy and R. C. Eberhart. Conf.: IEEE Intl. Conf. Systems, Man, and Cybernetics, Piscataway, NJ. IEEE, publ. (1997).
[24] R. Piestun and J. Shamir, "Synthesis of three-dimensional light fields and applications," *Proc. IEEE* **90**, pp. 222-244, (2002).
[25] J. L. Bakx, "Efficient computation of optical disk readout by use of the chirp z transform," *Appl. Opt.* **41**, pp. 4897-4903, (2003).
[26] H. Kim, B. Yang, and B. Lee, "Iterative Fourier transform algorithm with regularization for the optimal design of diffractive optical elements," *J. Opt. Soc. Am. A* **21**, pp. 2353-2365, (2004).